Manuscript Details

Manuscript number	MATERIALSCHAR_2019_439_R1
Title	THE EFFECTS OF MgO, Na2O AND SO3 ON INDUSTRIAL CLINKERING PROCESS: PHASE COMPOSITION, POLYMORPHISM, MICROSTRUCTURE AND HYDRATION, USING A MULTIDISCIPLINARY APPROACH.
Article type	Research Paper

Abstract

The present investigation deals with how minor elements (their oxides: MgO, Na2O and SO3) in industrial kiln feeds affect (i) chemical reactions upon clinkering, (ii) resulting phase composition and microstructure of clinker, (iii) hydration process during cement production. Our results show that all these points are remarkably sensitive to the combination and interference effects between the minor chemical species mentioned above. Upon clinkering, all the industrial raw meals here used exhibit the same formation temperature and amount of liquid phase. Minor elements are preferentially hosted by secondary phases, such as periclase. Conversely, the growth rate of the main clinker phases (alite and belite) is significantly affected by the nature and combination of minor oxides. MgO and Na2O give a very fast C3S formation rate at T > 1450 K, whereas Na2O and SO3 boost C2S. After heating, if SO3 occurs in combination with MgO and/or Na2O, it does not inihibit the C3S crystallisation as expected. Rather, it promotes the stabilisation of M1-C3S, thus indirectly influencing the aluminate content, too. MgO increseases the C3S amount and promotes the stabilisation of M3-C3S, when it is in combination with Na2O. Na2O seems to be mainly hosted by calcium aluminate structure, but it does not induce the stabilisation of the orhtorhombic polymorph, as supposed to occur. Such features play a key role in predicting the physical-mechanical performance of a final cement (i.e. rate of hydration and hardening) when used as a bulding material.

Keywords	minor elements; clinker; cement; hydration; polymorphism;

Corresponding Author	Nicoletta Marinoni
Corresponding Author's Institution	University of Milan
Order of Authors	Monica Segata, Nicoletta Marinoni, Matteo Galimberti, Maurizio Marchi, Marco Cantaluppi, Alessandro Pavese, Ángeles G. De la Torre
Suggested reviewers	Alberto Viani, Paulo Monteiro, Miguel A.G. Aranda, Gilberto Artioli

Submission Files Included in this PDF

File Name [File Type]

Response to Reviewers.docx [Response to Reviewers]

Cover Letter.docx [Highlights]

Highlights.docx [Highlights]

Revised text.docx [Manuscript File]

Figure 1_revised.tif [Figure]

Figure 2.tif [Figure]

Figure 4.tif [Figure]

Figure 5.tif [Figure]

Figure 6_revised.tif [Figure]

Figure 7.tif [Figure]

Figure 8.tif [Figure]

Figure 9.tif [Figure]

THE EFFECTS OF MgO, Na_2O AND SO_3 ON INDUSTRIAL CLINKERING PROCESS: PHASE COMPOSITION, POLYMORPHISM, MICROSTRUCTURE AND HYDRATION, USING A MULTIDISCIPLINARY APPROACH.

Monica Segata[a], Nicoletta Marinoni[b,c*], Matteo Galimberti[b], Maurizio Marchi[a], Marco Cantaluppi[b], Alessandro Pavese[d], Ángeles G. De la Torre[e]

[a] Global Product Inoovation (GPI) Department – Italcementi S.p.A. – Heidelbergcement Group, Bergamo, Italia

[b] Dipartimento di Scienze della Terra "Ardito Desio", Università degli Studi di Milano, Milano, Italy

[c] CNR (Consiglio Nazionale delle Ricerche)-IDPA, Milano, Italia

[d] Dipartimento di Scienze della Terra , Università di Torino, Torino, Italia

[e] Departamento de Química Inorgánica, Cristalografía y Mineralogía, Universidad de Málaga, Málaga, Spain

* Corresponding author

E-mail address: nicoletta.marinoni@unimi.it

Abstract

The present investigation deals with how minor elements (their oxides: MgO, Na_2O and SO_3) in industrial kiln feeds affect (i) chemical reactions upon clinkering, (ii) resulting phase composition and microstructure of clinker, (iii) hydration process during cement production.

Our results show that all these points are remarkably sensitive to the combination and interference effects between the minor chemical species mentioned above.

Upon clinkering, all the industrial raw meals here used exhibit the same formation temperature and amount of liquid phase. Minor elements are preferentially hosted by secondary phases, such as periclase. Conversely, the growth rate of the main clinker phases (alite and belite) is significantly affected by the nature and combination of minor oxides. MgO and Na_2O give a very fast C_3S formation rate at $T > 1450$ K, whereas Na_2O and SO_3 boost C_2S.

After heating, if SO_3 occurs in combination with MgO and/or Na_2O, it does not inihibit the C_3S crystallisation as expected. Rather, it promotes the stabilisation of M_1-C_3S, thus indirectly influencing the aluminate content, too. MgO increseases the C_3S amount and promotes the stabilisation of M_3-C_3S, when it is in combination with Na_2O. Na_2O seems to be mainly hosted by calcium aluminate structure, but it does not induce the stabilisation of the orhtorhombic polymorph, as supposed to occur. Such features play a key role in predicting the physical-mechanical performance of a final cement (*i.e.* rate of hydration and hardening) when used as a bulding material.

Keywords: minor elements; clinker; cement; hydration; polymorphism.

1. Introduction

OPC industry is known to be very energy-consuming and air-polluting because a huge consumption of natural resources and a high input of energy due to the thermal treatment up to 1700 K are usually needed. The sintering of 1000 kg of clinker requires 850000 kcal, 1700 kg of raw materials and emits 850 kg of pollutants, mainly carbon dioxide (CO_2) [1,2].

Recently, an attractive approach to save energy is provided by the use of alternative materials, such as industrial wastes (i.e. blast-furnace slags or other industrial by products) that can be introduced as components of the kiln feed, partially substituting the standard clinker raw meal components. Wastes are highly appreciated because they decrease the clinkering temperature and accelerate the sintering reactions [3].

Although the recycle of these materials has become a common practice in cement industry, cautions must be taken because they can contain elements that, even at low concentration, remarkably affect the sintering process [4]. Minor elements can (i) enter the structure of the clinker phases forming different solid solutions (C_3S_{ss}, C_2S_{ss}, C_3A_{ss}, C_4AF_{ss} where "$_{ss}$" refers to solid solution) thereby affecting their polymorphic relationships or (ii) lead to the growth of unconventional phases (e.g. Zn-rich wastes lead to the crystallization of a new phase identified as $Ca_6Zn_3Al_4O_{15}$ in clinker) [5]. Minor elements induce severe effects on the grindability and hydration of the cement paste. For instance, the combined occurrence, even in trace, of Cu and Sn in the kiln feed causes a delay of the cement hydration, thus decreasing its early compressive strength [4].

SO_3, MgO and Na_2O are the most frequently existing minor components in industrial clinkers. The influence of individual ions/species has been broadly discussed. Several authors reported the influence of MgO on the clinker phase composition and microstructure [6 and references therein reported, 7,8,9,10], whereas the effects of SO_3 or Na_2O were investigated by [11,12,13,14].

On the contrary, the impact of combined foreign ions/species on the clinker formation and reactivity is still modestly explored [7,8,15,16,17,18,19]. All these studies investigated clinkers prepared from an appropriate mixture of analytical grade raw materials, and proved that the final clinker reactivity is difficult to be predicted because it depends on the mutual interaction of the different ions/species [6,20,21].

Even fewer studies have been published on the effects of combined ions/species in clinkers prepared from industrial kiln feeds and industrial-grade raw materials (limestone, clay and oxides) [22,23]. No research, to our knowledge, has been devoted to investigate the influence of the triplet MgO-SO_3-Na_2O on clinker burning and final reactivity.

In the light, in present research we aim to investigate how the simultaneous occurrence of two of these foreign oxides in industrial kiln feeds influences (i) the clinkering reactions, (ii) the mineralogical properties (*i.e*. polymorphism and microstructures) of the final clinker and (iii) the reactivity and hydration of the resulting cements.

This study was carried out on four raw meals: a reference mixture (*Mix_00*) with a composition close to the one of the standard OPC clinker; three other mixtures, prepared by mixing *Mix_00* with a combination of two dopants (i.e. MgO and Na_2O, Na_2O and SO_3, MgO and SO_3 respectively).

In this light, for the first time, the use of *in situ* high temperature X-ray powder diffraction (HT-XRPD) allows one to follow the solid state reactions, liquid phase appearance, polymorphic transformations that occur during clinker formation. This technique is widely used in materials science [24,25], whereas a few researches report *in situ* studies for cements [26,27,28]. By combing the *in situ* HT-XRPD with Rietveld method we obtained an accurate phase analysis as a function of temperature.

Furthermore, burnability tests were performed on the four selected raw meals. The obtained clinkers were investigated by means of *ex situ* XRPD and Rietveld Quantitative Phase Analysis (RQPA) was carried to determine their phase composition. The distribution of dopants in the crystal structures of the main phases was determined by means of an Electron Probe Micro-Analyser. Scanning Electron Microscopy (SEM) was used to investigate the microstructures occurring in the final clinker.

Finally, the use of isothermal conduction calorimetry measurements was performed to correlate the phase assemblage, polymorphism and microstructure with the hydration behaviour of the obtained clinkers.

2. Sample preparation

An industrial raw meal (*Mix_00)* with Lime Saturation Factor (LSF), Silica Modulus (SM) and Alumina Modulus (AM) values at 94.75, 2.62 and 1.69 respectively (Table 1), was used. Moreover, Natural dehydrate calcium sulphate (“Lages” calcium sulfate BNR), and certified chemical compounds, magnesium and sodium carbonates (Carlo Erba Reagents), were added to the industrial raw meal to produce three extra mixes (*Mix_MN*, *Mix_NS* and *Mix_MS*) with different Na_2O, SO_3 and MgO, Table 1.

Mix_00 has a composition close to that of an average Ordinary Portland Cement (OPC) clinker, whereas *Mix_MN, Mix_NS* and *Mix_MS* refer to raw meals doped with MgO + Na_2O, Na_2O + SO_3 and MgO + SO_3, respectively. Once prepared, they were homogenized in an automatic shaker for 120 min; all the used materials were powders with a grain size below 80 µm in order to guarantee the optimal reactivity during the burning process.

3. Experimental

3.1 In situ High Temperature and ex-situ X-ray Powder Diffraction (XRPD)

In-situ HT-XRPD measurements were performed by means of a Philips X'Pert diffractometer, in θ-θ Bragg-Brentano geometry, equipped with the AHT-PAP1600 furnace operating at a maximum temperature of 1700°C. The diffractometer is equipped with Cu-Kα radiation with a secondary monochromator with a sealed proportional counter detector.

Data were recorded from room temperature (RT) to 1700 K, every 50 K with a heating rate of 30°/min. At 1700 K the samples were maintained for 45 minutes to achieve full clinkerization. The patterns were collected in the angular range of 5-70° (2θ), with a 0.03° of step size and a counting time of 0.8 s/step. These conditions allowed a quick data collection, in order to reduce the time spent on isothermal conditions but, at the same time, to preserve a counting statistics for a reliable RQPA.

Ex-situ XRPD experiments allowed one to investigate the clinker mineralogy and polymorphs assemblage in clinker after burning test. Data collections were carried out by an X'Pert PRO Diffractometer (PANalytical), in θ-2θ Bragg-Brentano geometry, equipped with an X'Celerator LPS detector. The 5–70° 2θ angular range has been investigated using Cu-Kα radiation, 40 kV current tension, 40 mA current intensity, 0.02° step size and an equivalent counting time of 50 s/step referred to a standard detector.

A preliminary phase identification on *in-situ* and *ex-situ* patterns was performed by means of PANalytical X'Pert High Score Plus 2.1.2 software, referring to ICDD database. The RQPA was obtained by the use of TOPAS-Academic 5.1 software [29]. Table 2 shows the structural descriptions for crystalline phases used during Rietveld refinement.

3.2 Burnability Test

5 g of each raw mixture were pressed under 4 kN into pellets, which were then fired in a vertical tube furnace (RHF 16/35 Carbolite).

Before entering the furnace, the pellets were placed in sealed platinum crucibles in order to prevent the loss of volatile elements during the firing process and successively calcined at 1200 K for 30 min. Clinkering was performed by heating the pre-calcined pellets at 1700 K for 45 min, cooling them down to 1600 K and finally quenching them to room temperature with a pressurized air flow. The obtained clinkers are hereafter addressed to as *Clinker_x* where *x* refers to the minor elements used as dopants (*i.e.* *x = 00*, *MN*, *NS* and *MS,* respectively).

3.3 Electron Probe Micro-Analyser

The main clinker phases were examined using an electron probe micro-analyzer (EPMA, Jeol 8600) (Model JEOL 8600) with an accelerating voltage of 15 keV, a beam current of 10 nA and an electron probe spot size of 1μm. All phases were analysed for Si, Al, Fe, Ca, Mg, S, Na, K, Ti, Cr, Mn and Sr using silicate and oxide standards and using ZAF correction. C_2S and C_3S were identified according to the SiO_2 content and CaO/SiO_2 weight ratio. Spot analyses on C_4AF departed remarkably from stoichiometry and were discarded because of crystals lacking size sufficient for reliable analyses (average size < 1μm).

Statistical analysis of the individual spot compositions was performed by calculating the correlation matrix from the spot analysis sets of alite and belite, using the Pearson-product-moment correlation.

3.4 Scanning Electron Microscopy

Small pieces of pellets of some clinkers were mounted in epoxy resins and were progressively diamond polished down to 3 μm. Finally, a mechanical etching with 0.3 μm alumina paste was applied in order to create contrast among different phases.

Polished sections of the clinker obtained after burnability test were investigated by means of a Zeiss EVO MA15 scanning electron microscope (SEM, Zeiss EVO MA15), operating with an acceleration current of 15 kV, a beam size of 100 nm and a working distance of 11 mm; the image resolution is 1024 x 730 pixels. Attention was paid to the clinker microstructures, such as the grain size, shape of silicate and aluminate phases.

3.5 Heat-Flow Calorimetric Analysis

For the calorimetric study, cements were prepared by mixing industrial gypsum to the selected clinkers to attain the same SO_3 value (~3.20 wt%).

The obtained pastes (2 g of cement with a cement to water ratio of 0.4) were equilibrated to temperature, mixed by hand for 2 min in a plastic beaker, and then transferred to the heat-flow calorimeter for 24 hours at 20 °C using a TAM Air instrument. Each experiment was repeated 3-4 times to verify reproducibility, and the results here shown are the average values of the measurements on such sets. The obtained cements are hereafter labelled as *Cement_x* where *x* refers to the minor elements used as dopants (*i.e*. *x* = *00*, *MN*, *NS* and *MS,* respectively).

4. Results

4.1 In-situ High Temperature X-Ray Powder Diffraction Analysis (In situ HT-XRPD)

HT-XRPD patterns allow one to obtain an insight of the main reactions taking place during clinkering and follow the polymorphic transformations of the clinker phases. Fig. 1 shows a selected range of

XRPD patterns collected during *in situ* HT-XRPD experiments for *Mix_NS* as an example. Fig. 2 shows a representative example of the Rietveld plots of the *in-situ* study.

At T < 1200 K all samples contain $\alpha'_L C_2S$, CaO, SiO_2 and anorthite, but dissimilarities occur in the phases weight fractions (*i.e.* CaO is ~36 wt% in *Mix_00* and ~75 wt% in *Mix_MS*). Periclase, anhydrite and natrite (Na_2CO_3) appear as minor phases, but in *Mix_00.*

At T > 1200 K, the phase composition as a function of temperature is reported in Fig. 3, where the liquid component was indirectly determined from the highest C_3A and C_4AF wt% values just before their melting [28].

A linear regression was used to model the relationship between the calcium silicate phase amounts and the different firing temperatures (T_f). In Table 3 the slope values (expressed as the angular coefficient m of the trend line) for the main silicate phases (m_x where x is C_2S, CaO and C_3S respectively) as a function of T_f are reported. These slopes can be directly compared with each other because the heating rates and the isothermal stage durations were the same for all the data collections.

An inspection of Fig. 3 and Table 3 suggests to divide the sequence of clinkering into three different steps:

step I (temperature range 1200-1400 K): a solid state reaction region before the appearance of C_3S, where CaO reacts with the alumina or silicate phases to form C_2S, C_4AF and C_3A.

The phase assemblage of *Mix_00* and *Mix_MN* consists of free lime, C_2S, C_4AF and C_3A associated to small amount of remaining SiO_2. Conversely, in *Mix_MS* and *Mix_NS* C_3A does not appear until *the mix* reaches 1350 K.

In this temperature range the phase transformation of C_2S from α'_H to α occurs [32].

step II (temperature range 1400-1450 K): a solid state reaction region where C_3S develops from a solid state reaction between C_2S and CaO.

The highest content in this temperature range of C_3S is observed in the reference mixture, although it appears at a low percentage. The presence of this phase, especially in *Mix_MN, is* negligible.

Moreover, the foreign ions induce structural modification of C_3A, as expected: in *Mix*_00 it is cubic, in *Mix_MN* and *Mix_NS* the orthorhombic form appears whereas the two polymorphs coexist in *Mix_MS* [12,13,44].

step III (temperature range 1450-1700 K): liquid reaction region where C_3S grows in presence of a liquid phase, as described in [12].

At 1450 K the aluminates melt, as suggested by the appearance of a liquid phase at the same temperature in all the samples. The presence of this melt favours the reaction of belite with CaO to form alite, even at a faster rate with respect to the reference, especially in *Mix_MN* and *Mix_MS,* mainly due to its lower viscosity due to the presence of minor elements [45]. In *Mix_NS,* there is not total consumption of CaO mainly due to the presence of Na_2O that substituted calcium in aluminates (Table 3). At this point is worthy pointing that the RQPA results of high temperature seems to contain artifacts such as slightly increasing amounts of CaO (in *Mix_NS* at 1550 K) or C_2S (in *Mix_NS* and *Mix_MN* at 1650 K). These artifacts may be indicating that the assumption of constant amorphous/melted fraction is not consistent anymore. However, the deviations are small enough to follow the effect of minor elements in the clinkering which is the main aim of this work.

In the doped samples, the amount of C_3S is higher at lower temperatures with respect to the reference sample. However, at 1700 K the C_3S content achieves a common value in all the investigated meals, i.e. ~80 wt%.

4.2 Ex situ Quantitative X-Ray Powder Diffraction Analysis (Ex situ QXRPD)

Table 4 gives the results of the *ex situ* RQPA of the clinkers. Fig. 4 shows, as an example, the Rietveld plots of *Mix_NS.*

On the one hand, from Table 4, it is concluded that silicates (alite and belite) have been affected mainly by Mg and sulphur, as discussed in previous studies [7,13-16]. In *Clinker_MN*, an increase in the amount of total C_3S is observed, jointly with a decrease of C_2S content from ~14 wt% in *Mix_00* to ~6 wt%, as expected [8], due to the substitution of Ca by Mg in alite. On the other hand, total alite content has decreased in those clinkers with some sulphur in their compositions, *i. e. Clinker_MS* and *Clinker_NS*, being a greater decrease in the one without magnesium. This was also an expected effect as sulphur has an overall positive effect on the crystallization of C_2S, as already reported in [7,8,13-17].

In addition, sulphur and magnesium has also an impact on alite polymorphism. In particular, those clinkers with higher amounts of sulphur, presents higher amounts of M_1 polymorph [8], while MgO (*Clinker_MN*) lead to the stabilization of M_3 C_3S (Fig. 5). In the present study the distinction between the different polymorphs becomes evident when looking at the angular windows in the XRPD patterns as described by [12,30,46].

On the other hand, sulphur tends to cause a decrease of the C_3A weight fraction (with respect to the standard *Clinker_00*), *Clinker_MS* and *Clinker_NS.* Moreover, C_4AF is favoured to crystallize in clinker with magnesium and sulphur.

Further consequences on clinker mineralogy include variations in the polymorphs of the main clinker phases (Fig. 5). In particular, MgO and Na_2O (*Clinker_MN*) lead to the stabilisation of M_3 C_3S and to the coexistence of the two polymorphic phases of C_3A, of which the orthorhombic one is dominant [7,12]. On the contrary, in *Clinker_NS* C_3S prefers M_1 with respect to M_3 and the cubic phase of C_3A

is bar far more relevant than the orthorhombic one. *Clinker_MS* behaves similarly to *Clinker_MN*, as for C_3S and to *Clinker_NS* as for C_3A.

4.3 Chemistry of clinker phases by means of EMPA

In Table 5 we show the chemical composition of C_3S, C_2S and C_3A in the suite of the clinkers investigated. The reported results are the averages of 20-30 individual spot analyses for each clinker; e.s.d.s are between brackets.

On the whole, both calcium silicates and aluminates accommodate nearly all the minor elements added to the *Mix_00*. In *Clinker_MN*, Mg^{2+} is mostly incorporated in the C_3S structure even if Mg-rich C_2S and C_3A/C_4AF phases are observed [6]. Na_2O is noticeably higher in aluminates, mainly in C_3A, than elsewhere, but the incorporation of Na^+ ions in the C_3S crystal lattice also occurs [6,47].

In *Clinker_NS* sulphur exhibits a preference for belite whereas sodium is mainly incorporated in the C_3A structure, even if a slight content of Na_2O is also revealed in C_2S. An increase of Al_2O_3 and a decrease of K_2O take place in C_3S and C_2S structures [6,47].

In *Clinker_MS* high contents of sulphur are detected in C_2S and C_3A, whereas magnesium enters both C_3S and C_3A phases. An increase in Al_2O_3 content is observed in C_2S. On the other hand, high contents of Al_2O_3 and SO_3 (~ 1.3 and ~ 0.30 wt% respectively) are observed in several C_3S crystals [6,47].

Fig. 6 shows the partitioning of the minor oxides between alite and belite in different clinkers. MgO mostly concentrates in alite, whereas SO_3 and Na_2O mainly enter belite. FeO and Al_2O_3 do not exhibit an apparent preference, although seem to have a slight penchant for belite.

A statistical analysis on the EMPA results allows one to determine the correlation degree between the concentrations of the individual element in the clinker phases (Table 6). In alite, we find inverse correlations between MgO-CaO, and between SiO_2-Al_2O_3; a positive correlation holds between Al_2O_3-Fe_2O_3. In belite, a positive correlation between Al_2O_3-Fe_2O_3, and an inverse correlation between SiO_2-SO_3 occur, at variance with what takes place in alite. No correlations were detected in C_3A crystals.

4.4 Microstructural analysis by means of SEM

In the reference clinker, alite crystals dominate the sample texture, with particle size ranging from 20 to 30 µm; they have prismatic habit with a slightly rounded hexagonal outline. Belite crystals were uniformly dispersed and appear as small roundish grains, having a size of approximately 10-20 µm, surrounded by an interstitial matrix (Fig. 7a).

In *Clinker_MN*, alite exhibits a bimodal distribution, where large crystals up to 30 µm with an irregular shape are associated to smaller ones (~ 5-10 µm), the latter displaying more regular faceted shapes and attributable to M_3 polymorph (Fig. 7b). Evidences of C_2S and aluminate inclusions within the largest C_3S crystals, as well as C_2S crystals with a complex lamellar structure, are present. The silicate crystals appear embedded in an aluminate matrix where C_3A and C_4AF are finely intergrowth. In *Clinker_NS*, M_1 C_3S crystals are irregular in shape and have the largest size (~ 100-200 µm) among all samples. Small and rounded grains of β-C_2S with subparallel cracking are observed. Crystals with a complex lamellar structure appear as a consequence of the α' belite stabilisation. All the silicates are embedded in an aluminate matrix (Fig. 7c).

Finally, in *Clinker_MS*, a dense-packed array of idiomorphic C_3S crystals (~ 50-100 µm), with associated rounded C_2S grains, both with a grain size similar to the one observed in *Clinker_00*, occurs. The interstitial matrix differs significantly from that of a conventional clinker owing to a higher amount of micrometric C_4AF crystals with a dendritic morphology. In addition, the packing of the silicate grains is so dense that little interstitial phase can exist between them (Fig. 7d).

4.5 Calorimetric study

A comparison of the hydration behavior was made by calorimetric measurements of the different samples and reported in Fig.8. The normalized heat flow curves highlight different behavior towards reactivity of the four investigated cements. In particular *Cement_NS* and *_MS*, which have a higher content in M_1 C_3S form exhibit as higher heat in the induction period (that is from the contact with water up to the starting of the accelerating period) than *Cement_00* and *_MN*. On the other hand, the acceleration period starts in shorter time if compared with *Cement_00* and *_MN* (3 h *versus* 3.5 h respectively) with also a more rapid increase in the heat flow. Finally, *Cement_MN* exhibits a later increase of the heat flow after 24 hours.

5. Discussion

A recent review on cement clinker chemistry clarifies the influence of minor and trace elements on clinker formation [6,48] and the conclusions are summarised in Fig. 9. MgO favours the growth of M_3 alite at the expenses of belite, whereas no variation in the interstitial phase amount occurs. In contrast, an increase of the Na_2O amount facilitates the growth of belite and affects the relationships between polymorphs, stabilizing M_1 C_3S and the orthorhombic C_3A [12]. SO_3 boosts the content of belite and ferrite at the expenses of alite and C_3A, promotes the occurrence of the M_1 C_3S and lowers the temperature of the liquid phase formation [13].

Note that in the present discussion, the notation C_3S and C_2S is used for pure calcium silicate phases (i.e. alite and belite); when discussing the effects of the incorporation of foreign ions in the alite and belite structures (i.e. solid solution) we refer to C_3S_{ss} and C_2S_{ss} respectively.

The *HT-XRPD* results highlight that foreign ions do not have an impact on the first step of the clinkerization (*Step I* of Fig. 3). Each foreign ion is not incorporated into clinker phases, rather it favours the growth of a secondary phase. Mg leads to periclase, sodium and sulphur promote natrite and anhydrite, respectively. The simultaneous presence of sodium and sulphur does not seem to induce the crystallisation of alkaline sulphates (*i.e.* aphthitalite), as usually reported in literature [22,23].

In *Step II* of Fig. 3 natrite and anhydrate dissolve away whereas periclase still remains preserved as a crystalline phase. In *Mix_MS* $CaSO_4$ decomposes at 1450 K and sulphur ions seem to be preferentially entrapped into C_2S_{ss}, whose content amounts to ~ 57 wt%.

In *Mix_NS* Na_2CO_3 acts as flux, reducing the temperature at which $CaSO_4$ melts. S^{VI} ions are thus available at 1400 K, thus boosting the C_2S_{ss} rate of growth and content (up to ~ 57 wt%) at lower *T* in comparison with *Mix_MS*.

The sulphur incorporation in the C_2S_{ss} crystal structure cannot be a simple isomorphous substitution, and it is usually described through a complex replacement involving other chemical species [6,12,47]. In particular, the substitution of Si^{IV} with S^{VI} is facilitated by a concomitant Al^{3+} substitution on the same site (*i.e.* 3 $Si^{IV} \Leftrightarrow S^{VI} + 2\ Al^{3+}$), as confirmed by a sulphate concentration in C_2S_{ss} crystals larger than that in alite. These substitutions decrease the content of Al_2O_3, thus leading to a reduction of C_3A. C_3A growths when starts the C_2S_{ss} decomposition, which makes aluminium available for belite formation. The unit cell value of β-C_2S_{ss} gives an idea of the degree of inclusion of foreign elements in its structure [49]. The published unit cell volume of stoichiometric belite is 345.8 $Å^3$ [32] while in *Clinker_MS and Clinker_NS* C_2S_{ss} shows expanded unit cells of 348.7 $Å^3$ and 348.8 $Å^3$, respectively, as a consequence of the inclusion of sulphur and aluminium in the structure. Na^+ ions are preferentially incorporated into the aluminates, causing a stabilisation of the orthorhombic polymorph of C_3A in *Mix_MN* and *Mix_NS,* respectively.

In *Step II* C_3S appears through a solid state reaction between C_2S_{ss} and CaO but the foreign ions do not influence its growth as one would expect. In particular, the lowest contents of C_3S_{ss} are observed in *Mix_MN*, where Mg^{2+} ions concentrate in periclase and cannot contribute to alite growth.

With increasing firing temperature (*Step III* of Fig. 3), all foreign ions dissolve in the melt and have a strong impact on the physical properties of the liquid phase but, in these experimental conditions, foreign ions affect neither its temperature of first appearance nor amount, as usually expected in the presence of MgO and SO_3 [7,16,17,50,51]. These latter species presumably cause a decrease of viscosity and enhance the wettability of the liquid phase, thus accelerating the rate of growth of alite. In the doped mixtures m_x of alite has higher values than in the reference (*i.e.* m_x ~ 0.39 *vs* ~ 0.50 in *Mix_00* and *Mix_MN*, respectively), resulting in high contents of C_3S_{ss} in *Mix_MN* due to the incorporation of Mg^{2+} ions into its structure. It is apparent the stabilisation effect of SO_3 on belite at the expenses of C_3S_{ss}, as shown by a comparison of the alite contents in *Mix_MS* and *Mix_00*.

In *Mix_NS* the high content of CaO at 1700 K might be considered as the result of the C_2S_{ss} decomposition (Table 3). As previously mention, in this sample the liquid phase is Al-depleted due to the incorporation of S^{VI} and Al^{3+} into the belite structure; this provides a high wettability and low viscosity of the liquid phase that can easily interact with the C_2S_{ss} crystals, thus favouring their decomposition with a consequent release of CaO.

Eventually, the clinkerisation ends up with a fast cooling where the foreign ions presumably redistribute among the clinker phases, thus influencing the mineralogy and microstructure of the final clinkers as well as their hydration behaviour.

In particular, the *ex-situ* results confirm that Mg^{2+} ions, even if in combination with other ions, are preferentially incorporated in alite structure. The highest content of small and well faceted M_3 C_3S_{ss} highlighted by XRPD and SEM in *Clinker_MN* would suggest the occurrence of Mg^{2+} ions in C_3S_{ss} crystals. EMPA results confirms that C_3S forms solid solution with magnesium that enters alite up to ~ 1.30 wt%. No relevant change of Al_2O_3 and SiO_2, contents are observed. All this suggests that a replacement takes place between magnesium and calcium in the octahedral site of the silicate phases.

In *Clinker_MS* MgO compensates the negative effect that would exert SO_3 on C_3S_{ss} formation. Mg^{2+} ions are fully entrapped in alite crystals, favouring the growth and stabilisation of M_3 polymorph. EMPA results confirm the substitution between Mg^{2+} and Ca^{2+} in C_3S_{ss}.

The contents of SO_3 and Al_2O_3 exhibited by several C_3S_{ss} crystals suggest that two additional substitutions can occur:

(i) the replacement of Si^{IV} with S^{VI} and Al^{3+}, as already described for C_2S_{ss} crystals;

(ii) a partial substitution of silicon with aluminium in the tetrahedral crystal site and a simultaneous removal of Na^+ or K^+ ions, probably located into the interstitial lattice sites according to the reaction $2\ K^+ + Si^{IV} \Leftrightarrow 2\ Al^{3+}$. The K_2O and Al_2O_3 contents highlighted during EMPA analyses confirm this latter hypothesis.

The presence of Al^{3+} and S^{VI} might be responsible for the stabilisation of M_1 C_3S_{ss}. Therefore, we can assert that the combined presence of MgO and SO_3 seems to be the driving factor for the stabilization of the alite M_1 polymorph. In particular, a low value of MgO/SO_3 encourages the stabilization of the structural modification M_1 [52].

In *Clinker_MS* and *_NS* it is confirmed the key role of sulphur on C_2S_{ss} growth. As reported in literature, the crystallisation of high amounts of large crystals of belite and the stabilisation of the beta polymorph is encouraged in the presence of SO_3 [7,8,16,48].

Furthermore, it seems that the combined presence of dopants strong impacts onto the interstitial phase formation. In particular, the effects of two dopants on the aluminate crystallisation could not be predicted by considering the effects of each single dopant. In the presence of Na_2O and SO_3, the high contents of Al_2O_3 entrapped into calcium silicates result in a general reduction of the Al_2O_3 amount in the liquid phase, leading to a reduction of C_3A content in the final clinker. Na^+ ions are entrapped into the calcium aluminate structure but do not induce the stabilization of the orthorhombic polymorph, as one would have expected.

The simultaneous presence of SO_3 and MgO reduces the phase content of C_3A but increases the one of C_4AF. The stability range of C_3A in the phase diagram CaO-SiO_2-Al_2O_3-Fe_2O_3 is reduced and the peritectic reaction $L + C_3S \rightarrow C_2S + C_3A$ does not occur whereas $L + C_2S \rightarrow C_3S + C_4AF$ seems to be promoted, thus leading to high content of ferrite phase at the expenses of C_3A [53].

Finally, the calorimetry results remark that predicting the reactivity towards hydration on cements relying on a single microstructural feature (i.e. mineralogy, polymorphism or microstructure) and/or dopant contents (minor oxides contents in the crystalline phases) is a difficult task. Rather we might suppose that the effects of each single feature do not sum additively but interact among them making thus impossible to determine unequivocally the overall cement reactivity towards hydration. As a whole, a higher reactivity towards hydration in *Cements_NS* and *_MS* is highlighted by a shorter induction period with respect to *Cement_MN* and *_00,* suggesting that the presence of M_1 C_3S_{ss} might shorten and speed up the acceleration period. This increase in reactivity may also be related to the higher strengths of M_1 containing cements observed by other authors [53]. On the other hand, we cannot exclude that the larger crystal size of calcium silicates highlighted by SEM investigations as well as the presence of alkali sulphate detected by means of *ex situ* XRPD in *Clinkers_NS* and *_MS* have also a key role on the overall hydration [13-19]. Again, it seems that the setting regulator dissolution is affected by the presence of alkali sulphate, leading to a modification of the pore solution composition, which is a fundamental factor in regulating the start of the acceleration period. On the contrary, in *Clinker_MN and _00* the high contents of M3 C_3S_{ss} with a smaller crystal size as well as the absence of alkaline phases promote the heat release from the contact with water up to the starting of the acceleration period, resulting in a higher heat release during the induction period only.

6. Conclusions

The clinkering reactions of four selected raw meals containing a combination of two minor elements have been investigated by means of *in situ* and *ex situ* XRPD and imagining techniques. The research aim is to clarify the effects of MgO-Na_2O, Na_2O-SO_3, SO_3-MgO on the clinkering process in terms of final clinker mineralogical, microstructural and hydration properties. Our results show that minor species:

✓ do not influence the temperature of appearance and amount of the liquid phase, as usually reported to occur in presence of MgO and/or SO_3;

✓ promote the rate of growth for C_2S_{ss} during solid state reaction (*step I* and *II* of Fig. 3) as well as improve the growth rate for C_2S_{ss} and CaO in presence of a liquid phase (*step III* of Fig. 3);

✓ reduce the C_3S_{ss} formation during solid state reaction (*step II* of Fig. 3). In the MgO and SO_3-bearing mix the growth of C_3S_{ss} in the solid state region is inhibited. On the contrary, it is enhanced when the liquid phase appears. The raw meals produced with the addition of MgO result in the most rapid C_3S formation during the liquid phase region.

✓ SO_3 promotes the stabilization of M_1 polymorph of C_3S_{ss} independently on the other foreign ions.

Moreover:

✓ SO_3 decreases the amount of aluminium ions available for the C_3A formation because its preferentially incorporation in belite crystals, thus leading to a delay of C_3A crystallisation temperature. C_3A appears when the decomposition of C_2S_{ss} starts;

✓ SO_3 and Na_2O seem to enhance the burnability of the raw meal during the solid state reaction;

✓ strongly influence the final clinker reactivity towards hydration which depends on the type of C_3S polymorph, the calcium silicate grain size and, last but not least, the presence/absence of minor sulphate phases.

As a whole, the present results point out how the effects of the simultaneous presence of several dopants cannot be predicted by considering the influence of each minor element alone on the final clinker. The system CaO-SiO_2-Al_2O_3-Fe_2O_3, usually considered for the formation process of cement clinker, is remarkably modified when more minor elements simultaneously occur in the starting raw meal. In particular, they influence its burnability and the properties of the interstitial liquid, thus significantly affecting the polymorph phases' occurrence, their amounts and microstructures in the resulting clinkers as well as in the final hydration behaviour.

Funding sources
This research did not receive any specific grant from funding agencies in the public, commercial, or not-for-profit sectors.

References

[1] M.B. Bali, R. Saidur, M.S. Hossain, A review on emission analysis in cement industries, Renew Sustain Energy Rev. 15 (2011) 2252-2261.

[2] I. Amato, Concrete solutions, Nat. 494 (2013) 300-301.

[3] R.I. Iacobescu, Y. Pontikes, D. Koumpouri, G.N. Angelopoulos, Synthesis, characterization and properties of calcium ferroaluminate belite cements produced with electric arc furnace slag as raw material, Cem. Concr. Comp. 44 (2013) 1-8.

[4] N. Gineys, G. Aouad, F. Sorrentino, D. Damidot, Incorporation of trace elements in Portland cement clinker: Thresholds limits for Cu, Ni, Sn or Zn, Cem. Concr. Res. 41 (2011) 1177–1184.

[5] D. Herfort, G.K. Moir, V. Johansen, F. Sorrentino, H. Bolio Arceo, The chemistry of Portland cement clinker, Adv. Cem. Res. 22 (2010) 187-194.

[6] H.M. Ludwig, W. Zhang, Research review of cement clinker chemistry, Cem. Concr. Res. 78 (2015) 24-27.

[7] I. Maki, K. Fukuda, H. Yoshida, J. Kumaki, Effect of MgO and SO_3 on the impurity concentration in alite in Portland cement clinker, J. Am. Ceram. Soc. 75 (1992) 3163-3165.

[8] I. Maki, K. Goto, Factors influencing the phase constitution of alite in Portland cement clinker, Cem. Concr. Res. 12 (1982) 301-308.

[9] N.N. Katyal, S.C. Ahluwalia, R. Parkash, Solid solution and hydration behavior of magnesium bearing tricalcium silicate phase, Cem. Concr. Res. 28 (1998) 867-875.

[10] A. Palomo, F.P. Glasser, Solubility of magnesium oxide in selected cement clinker phases, Adv. Cem. Res. 2 (1989) 55-59.

[11] S. Uda, E. Asakura, M. Nagashima, Influence of SO_3 on the phase relationship in the system CaO-SiO_2-Al_2O_3-Fe_2O_3, J. Am. Ceram. Soc. 81 (1998) 725-729.

[12] H.F.W. Taylor, Cement Chemistry, Academic Press, London, 1990.

[13] S. Horkoss, R. Lteif, T. Rizk, Influence of the clinker SO_3 on the cement characteristics, Cem. Concr. Res. 41 (2011) 913-919.

[14] A. Hamou-Tagnit, S.L. Sarkar, The influence of varying sulphur content on the microstructure of commercial clinkers and the properties of cement, World Cem. 21 (1990) 389–393.

[15] X. Li, H. Huang, S. Ma, X. Shen, Statistical research on phase formation and modification of alite polymorphs in cement clinker with SO_3 and MgO, Constr. Build. Mater. 37 (2012) 548–555.

[16] X. Li, W. Xu, S. Wang, X. Shen, Effect of SO_3 and MgO on Portland cement clinker: Formation of clinker phases and alite polymorphism, Constr. Build. Mater. 58 (2014) 182-192.

[17] J. Strunge, D. Knoefel, I. Dreizler, Effect of alkalies and sulfur on the properties of cement Part III: effect of alkalies and sulfate on the properties of cement taking into account the alumina ratio and the lime standard, Zem. Kalk Gips. 39 (1986) 380-386.

[18] J. Strunge, D. Knoefel, I. Dreizler, Effect of alkalies and sulfur on the properties of cement Part II: effect of alkalies and sulfate on the properties of cement, taking into account the silica ratio, Zem. Kalk Gips. 38 (1985) 441-450.

[19] J. Strunge, D. Knoefel, I. Dreizler, Effect of alkalies and sulfur on the properties of cement. Part I. Effect of the sulfur trioxide content on cement properties, Zem. Kalk Gips. 38 (1985) 150–158.

[20] K. Kolovos, S. Tsivilis, G. Kakali, The effect of foreign ions on the reactivity of the CaO-SiO_2-Al_2O_3-Fe_2O_3 system Part II: Cations, Cem. Concr. Res. 32 (2002) 463-469.

[21] K. Kolovos, P. Loutsi, S. Tsivilis, G. Kakali, The effect of foreign ions on the reactivity of the CaO-SiO_2-Al_2O_3-Fe_2O_3 system Part I: Anions, Cem. Concr. Res. 31 (2001) 425-429.

[22] A. Emanuelson, S.A.R. Landa-Cánovas, S. Hansen, A comparative study of ordinary and Portland cement clinker from two different production units Part II: Characteristics of the calcium silicates, Cem. Concr. Res. 33 (2003) 1623-1630.

[23] A. Emanuelson, S. Hansen, E. Viggh, A comparative study of ordinary and Portland cement clinker from two different production units Part I: Composition and hydration of the clinkers, Cem. Concr. Res. 33 (2003) 1613-1621.

[24] N. Marinoni, S. Allevi, M. Marchi, M. Dapiaggi, A Kinetic Study of Thermal Decomposition of Limestone Using In Situ High Temperature X-Ray Powder Diffraction, J. Am. Ceram. Soc. 95 (2012) 2491-2498.

[25] N. Marinoni, A. Pagani, I. Adamo, V. Diella, A. Pavese, F. Francescon, Kinetic study of mullite growth in sanitary-ware production by in situ HT-XRPD. The influence of the filler/flux ratio, J. Eur. Ceram. Soc. 31 (2011) 273-278.

[26] M. Marchi, U. Costa, G. Artioli, Influence of SO_3 and MgO on clinker mineralogical composition: an in situ HTXRD study, Proc. of the 12th Int. Cong. Chem. Cem., Montreal Canada (2007).

[27] A.G. De la Torre**,** A.J. Cuberos, G. Alvarez-Pinazo, A. Cuesta, M.A.G. Aranda, In situ powder diffraction study of belite sulfoaluminate clinkering, J. Synchrotron Radiat. 18 (2011) 506-514.

[28] A.G. De la Torre, K. Morsli, M. Zahir, M.A.G. Aranda, In situ synchrotron powder diffraction study of active belite clinkers, J. Appl. Cryst. 40 (2007) 999-1007.

[29] A.A. Coelho, TOPAS-Academic, version 5.1 (Computer Software), Coelho Software, Brisbane (2012).

[30] A.G. De la Torre, R.N. De Vera, A.J.M. Cuberos, M.A.G. Aranda, Crystal structure of low-magnesium content alite: application to Rietveld quantitative phase analysis, Cem. Concr. Res. 38 (2008) 1261-1269.

[31] F. Nishi, Y. Takeuchi, I. Maki, Tricalcium silicate $Ca_3O(SiO_4)$: The monoclinic superstructure, Z. Kristallogr. 172 (1985) 297-314.

[32] W.G. Mumme, R.J. Hill, G. Bushnell-Wye, E. Segnit, Rietveld structure refinement, crystal chemistry and calculated powder diffraction data for the polymorphs of dicalcium silicate and related phases, Neues Jahrb. Mineral. Abh. 169 (1995) 35–68.

[33] P. Mondal, J.W. Jeffery, The crystal structure of tricalcium aluminate, $Ca_3Al_2O_6$. Acta Cryst. B31 (1975) 689–697.

[34] Y. Takeuchi, F. Nishi, I. Maki, Crystal chemical characterization of the $(CaO)_3(Al_2O_3)$ - (Na_2O) solid solution series, Zeitschrift fuer Kristallographie 152 (1980) 259-307.

[35] A.A. Colville, S. Geller S, The crystal structure of brownmillerite, Ca_2FeAlO_5, Acta Cryst. B27 (1971) 2311-2315.

[36] G. Natta, L. Passerini, Soluzioni solide, isomorfismo e simmorfismo tra gli ossidi dei metalli bivalenti. - 1. Sistemi: CaO-CdO, CaO-MnO, CaO-CoO, CaO-NiO, CaO-MgO. Gazzetta Chimica Italiana 59 (1929) 129-154.

[37] S. Sasaki, K. Fujino, Y. Takeuchi, X-ray determination of electron-density distributions in oxides, MgO, MnO, CoO, and NiO, and atomic scattering factors of their constituent atoms. Proc. of the Japan Acad. 55 (1979) 43-48.

[38] F.C. Hawthorne, R.B. Ferguson, Anhydrous sulphates. II. Refinement of crystal structure of anhydrite. Can. Mineral. 13 (1975) 289-292.

[39] F.F. Foit, D.R. Peacor, The anorthite crystal structure at 410 and 830 °C. Am. Miner. 58 (1973) 665-675.

[40] T. Barth, G. Lunde, Die Gitterkonstanten des Platinmetalle, Silber und Gold, Zeitschrift fuer Physikalische Chemie 121 (1926) 78-102.

[41] K. Okada, J. Ossaka, Structures of Potassium Sodium Sulphate and Tripotassium Sodium Disulphate, Acta Cryst. B36 (1980) 919-921.

[42] K. Ojima, Y. Nishihata, A. Sawada, Structure of potassium sulfate at temperatures from 296 K down to 15 K. Acta Cryst. Sect. B51 (1995) 287-293.

[43] D. Speer, E. Salje, Phase transitions in langbeinites I: Crystal chemistry and structures of K-double sulfates of the langbeinite type $M_2^{++}K_2(SO_4)_3$, M^{++}= Mg, Ni, Co, Zn, Ca, Phys. Chem. Miner. 13 (1986) 17-24.

[44] L Gobbo, L Sant'Agostino, Garcez L, C3A polymorphs related to industrial clinker alkalies content. Cem. Concr. Res. 34 (2004) 657-664

[45] Y Butt Y, V Timashev V, The mechanism of clinker formation processes and ways of modification of clinker structure. Sixth International Congress on the Chemistry of Cement, Moscow (1974) p. 9.

[46] M. Cortial, M.N. de Noirfontaine, F. Dunstetter, G. Gasecki, M. Signes-Frehel, Polymorphism of tricalcium silicate in portland cement: a fast visual identification of structure and superstructure, Powder Diffr. 18 (2003) 7-15.

[47] E Woermann, T hann, W Eysel, The substitution of alkalies in tricalcium silicates, Cem Concr Res 9 (1979) 701-711.

[48] M. Marchi, M. Segata, F. Scotti, Effect of minor elements on clinker mineralogy and reactivity, Proc. of the 36th Int. Cem. Microsc. Assoc., Milano Italia (2014).

[49] K. Morsli, A.G. De la Torre, M. Zahir, M.A.G. Aranda, Mineralogical phase analysis of alkali and sulfate bearing belite rich laboratory clinker, Cem. Concr. Res. 37 (2007) 639-646.

[50] MA Aldieb, HG Ibrahim, Variation of Feed Chemical Composition and Its Effect on Clinker Formation-Simulation Process. Proceedings of the World Congress on Engineering and Computer Science, San Francisco, 20-22 October 2010, 699-705.

[51] I Jawed, JSkalny, Alkalies in cement: A review I. Forms of Alkalies and their effect on clinker formation. Cem. Concr. Res. 7 (1977) 719-729

[52] T. Stanek, P. Sulovsky, The influence of the alite polymorphism on the strength of Portland cement, Cem. Concr. Res. 32 (2002) 1169-1175.

[53] D. Harrison, G.K. Moir, V. Johansen, The chemistry of Portland cement clinker, Adv. Cem. Res. 22 (2010) 187-194.

Captions of Figures

Figure 1. Two-dimensional view of a selected range of the *in situ* HT-XRPD patterns during clinker formation collected on heating from 1200 to 1700 K (sample *Mix_NS*) with main peaks labelled.

Figure 2. Rietveld plot for *Mix_NS* collected by means of *in situ* HT-XRPD at 1400 K.

Figure 3. *In situ* HT-XRPD results (wt.%) for the four investigated raw meals as a function of the temperature (only the main crystalline phases are included).

Figure 4. RQPA plot for *Mix_NS* collected by means of *ex situ* XRPD. Main peaks of the main clinker phases have been labelled.

Figure 5. Weight percentages of the different polymorphs for C_3S (M_1 and M_3 monoclinic polymorphs) and C_3A (orthorhombic and cubic polymorphs), determined by RQPA.

Figure 6. Minor oxides' concentrations in alite and belite, as averages from spot analyses, in the reference (*Mix_00*, empty symbols) and the doped clinkers (full symbols).

Figure 7. BSE images of the clinkers after the clinkering: (a) large and idiomorphic C_3S crystals immersed in a matrix of C_3A and C_4AF crystals finely intergrowth (*Clinker_00*); (b) bimodal distribution of alite crystals (the smaller and larger ones are labelled as C_3SI and C_3SII respectively in the dotter area) associated with belite and aluminate crystals (*Clinker _MN*); (c) large and irregular in shape crystals of alite (red dotted area) and rounded belite crystals highly fractured surrounded by an aluminate matrix where C_3A appears in large crystals (*Clinker_NS*); (d) prismatic alite crystals and rounded belite crystals, all surrounded by an aluminate matrix of C_4AF (blue dotted area) (*Clinker_MS*).

Figure 8. Normalised heat flow of the selected samples during calorimetric test.

Figure 9. The effects of minor elements on the content and polymorphism of the main clinker phases are reported. The dotted line refers to the clinker phase contents in *Mix_00* whereas *, ** and *** refer to the *Mix_00* doped with MgO, Na_2O and SO_3 separately [6,45].

Tables

Oxides	*Chemical Compounds / wt%*			*Mixes / wt%*			
	$CaSO_4$	**$MgCO_3$**	**Na_2CO_3**	***Mix_00***	***Mix_MN***	***Mix_NS***	***Mix_MS***
SiO_2	-	-	-	14.21	13.85	14.31	13.70
Al_2O_3	-	-	-	3.44	3.30	3.37	3.24
Fe_2O_3	-	-	-	2.01	1.92	1.99	1.93
CaO	33.43			42.80	41.13	41.81	40.93
MgO	-	43.68		0.77	2.21	0.8	2.17
SO_3	47.73	-		0.2	0.20	1.53	1.42
Na_2O	-	-	58.48	0.12	0.45	0.44	0.10
K_2O	-	-	-	0.58	0.58	0.55	0.53
SrO	-	-	-	0.11	0.11	0.10	0.10
Mn_2O_3	-	-	-	0.05	0.05	0.07	0.06
P_2O_5	-	-	-	0.08	0.08	0.08	0.08
TiO_2	-	-	-	0.13	0.13	0.19	0.14
L.o.I.	18.84	56.32	41.52	35.42	36.04	34.87	35.55
Sum	100	100	100	99.92	99.92	99.93	99.95

Table 1. Chemical composition of the industrial raw meal, certified chemical compounds and mixes used in the present study.

Phase		References	ICSD #
C_3S	$T_3(M_1)$	De la Torre et al., 2008 [30]	162744
	M_3	Nishi et al., 1985 [31]	64759
C_2S	α'_H	Mumme et al., 1995 [32]	81097
	β	Mumme et al., 1995 [32]	81096
C_3A	cubic	Mondal&Jefferey, 1975 [33]	1841
	orthorhombic	Takeuchi et al., 1980 [34]	100220
C_4AF		Colville&Geller, 1971 [35]	9197
CaO		Natta&Passerini, 1929 [36]	61550
MgO		Sasaki et al., 1979 [37]	9863
Anhydrite		Hawthorne&Ferguson, 1975 [38]	40043
Anorthite		Foit et al., 1973 [39]	22022
Platinum		Barth et al., 1926 [40]	64917
Aphitalite		Okada et al., 1980 [41]	26018
Arcanite		Ojima et al., 1995 [42]	79777
Ca-langbenite		Speer&Salje, 1986 [43]	40989

Table 2. Structural models of phases used for the Rietveld analyses of clinkers from *in situ* and *ex-situ* data.

	SOLID STATE REACTION REGION			LIQUID PHASE REACTION REGION	
	***Step I* (1200-1400 K)**		***Step II* (1450 K)**	***Step III* (1450-1700 K)**	
C_2S	m_x (1200-1400 K)	wt% at 1400 K	wt% at 1450 K	m_x (1450-1700K)	wt% at 1700 K
Mix_00	0.02	52.4(2)	39.9(2)	-0.26	0.6(2)
Mix_MN	0.06	51.7(2)	54.9(2)	-0.31	2.4(2)
Mix_NS	0.08	56.9(2)	57.3(1)	-0.37	1.2(2)
Mix_MS	0.05	50.4(2)	56.8(2)	-0.29	3.7(2)
C	m_x (1200-1400 K)	wt% at 1400 K	wt% at 1450 K	m_x (1450-1700K)	wt% at 1700 K
Mix_00	- 0.03	30.1(1)	18.5(3)	-0.11	-
Mix_MN	-0.05	33.5(2)	25.9(2)	-0.26	-
Mix_NS	-0.09	26.1(2)	19.8(2)	-0.09	6.7(2)
Mix_MS	-0.06	30.9(2)	23.3(2)	-0.15	-
C_3S			wt% at 1450 K	m_x (1450-1700K)	wt% at 1700 K
Mix_00			25.7(2)	0.39	84.1(2)
Mix_MN			2.2(1)	0.50	85.9(2)
Mix_NS			7.4(1)	0.46	76.3(2)
Mix_MS			9.3(2)	0.48	80.9(2)

Table 3. Growth rates of the main clinker phases, expressed by the slope of the trend line between their weights percentage values obtained by Rietveld refinement as a function of temperature (*in situ* HT-XRPD results)

Phase	***Mix_00***	***Mix_MN***	***Mix_NS***	***Mix_MS***
C_3S-M_1	26.2(2)	19.0(2)	48.9(2)	41.8(2)
C_3S-M_3	40.1(2)	52.2(2)	14.4(2)	22.5(2)
C_3S-Total	***66.3(2)***	***71.2***	***63.3(2)***	***64.3(2)***
β-C_2S	0.9(2)	0.4(2)	10.2(2)	12.9(2)
α'_H-C_2S	13.3(2)	5.7(2)	10.0(2)	4.6(2)
C_2S-Total	***14.2(2)***	***6.1(2)***	***20.2(2)***	***17.5(2)***
C_3A cubic	3.2(2)	1.7(2)	7.9(2)	3.6(2)
C_3A orthorhombic	6.6(2)	10.9(2)	0.2(2)	-
C_3A-Total	***9.8(2)***	***12.6(2)***	***8.1(2)***	***3.6(2)***
C_4AF	6.9(2)	5.9(2)	6.8(2)	12.2(2)
CaO	1.6(2)	1.4(2)	< 1	< 1
$Ca(OH)_2$	< 1	< 1	< 1	< 1
MgO	< 1	1.8(2)	< 1	< 1
arcanite	-	< 1	< 1	-
aphthitalite	-	-	< 1	< 1

Table 4. *Ex-situ* Rietveld quantitative phase analysis (wt%) of the main clinker phases after heating in a laboratory furnace at 1700 K for 45 min (*ex situ* XRPD results).

Clinker Phase	Chemical composition (wt%)												
C_3S	SiO_2	Al_2O_3	FeO	CaO	MgO	SO_3	Na_2O	K_2O	TiO_2	Cr_2O_3	MnO	SrO	**Total**
Clinker_00	24.4(5)	1.0(2)	0.7(1)	71.8(2)	0.69(7)	0.02(1)	0.09(3)	0.08(3)	0.18(3)	0.02(3)	0.09(3)	0.16(5)	99.24
Clinker_MN	25.3(3)	0.8(1)	0.5(1)	71.2(2)	1.20(1)	0.02(1)	0.20(3)	0.08(2)	0.16(5)	0.01(2)	0.08(4)	0.1(1)	99.77
Clinker_NS	24.5(3)	1.2(2)	0.6(1)	71.8(3)	0.71(5)	0.21(3)	0.08(2)	0.01(1)	0.18(4)	0.02(2)	0.07(3)	0.09(7)	99.44
Clinker_MS	24.3(3)	1.3(2)	0.6(1)	71.2(2)	1.28(7)	0.29(5)	0.03(2)	0.01(1)	0.18(6)	0.01(2)	0.0783)	0.09(7)	99.32
C_2S	SiO_2	Al_2O_3	FeO	CaO	MgO	SO_3	Na_2O	K_2O	TiO_2	Cr_2O_3	MnO	SrO	**Total**
Clinker_00	30.7(2)	1.65(9)	1.1(1)	63.0(3)	0.31(4)	0.19(3)	0.24(5)	0.88(3)	0.30(1)	0.01(1)	0.09(2)	0.20(1)	98.77
Clinker_MN	31.8(4)	1.40(1)	1.10(1)	62.1(5)	0.51(5)	0.15(4)	0.69(9)	0.84(5)	0.21(1)	0.01(3)	0.11(3)	0.31(1)	99.35
Clinker_NS	29.9(8)	2.01(2)	1.10(2)	63.2(3)	0.30(8)	1.40(2)	0.49(6)	0.17(2)	0.27(6)	0.01(2)	0.09(3)	0.22(1)	99.17
Clinker_MS	30.1(3)	2.11(1)	1.02(7)	63.1(5)	0.29(8)	0.54(8)	0.24(9)	0.44(4)	0.26(7)	0.02(2)	0.09(3)	0.32(2)	97.40
C_3A	SiO_2	Al_2O_3	FeO	CaO	MgO	SO_3	Na_2O	K_2O	TiO_2	Cr_2O_3	MnO	SrO	**Total**
Clinker_00	4.11(1)	24.6(3)	12.0(6)	53.3(7)	1.79(9)	0.02(2)	0.7(1)	0.7(2)	0.72(6)	0.02(2)	0.53(5)	0.20(1)	98.73
Clinker_MN	5.40(8)	23.3(9)	11.7(7)	51.1(4)	2.70(4)	0.01(1)	2.00(1)	1.00(2)	0.80(1)	0.01(2)	0.60(1)	0.24(7)	98.79
Clinker_NS	4.51(2)	23.5(9)	13.3(1)	52.9(4)	2.23(8)	0.13(2)	0.32(3)	0.04(3)	0.72(3)	0.02(1)	0.60(3)	0.19(7)	98.20
Clinker_MS	4.42(4)	24.9(3)	11.8(3)	53.0(1)	3.00(1)	0.29(4)	0.07(2)	0.03(2)	0.6(2)	0.02(3)	04(1)	0.20(8)	98.95

Table 5. Chemical composition of the main clinker phases (wt.%); standard deviation in parentheses.

Clinker phase	Correlation Coefficient*
Alite (n = 100)	
Mg, Ca	- 0.62
Al, Si	- 0.75
Si, Fe	+ 0.35
Belite (n=100)	
Al, Si	-0.74
Al, Fe	+0.58
Si, S	-0.68

Table 6. Correlation Coefficients between concentrations of oxides in the clinker phases. * The Correlation Coefficient is strongly significant if > 0.5, n is the sampling.

□

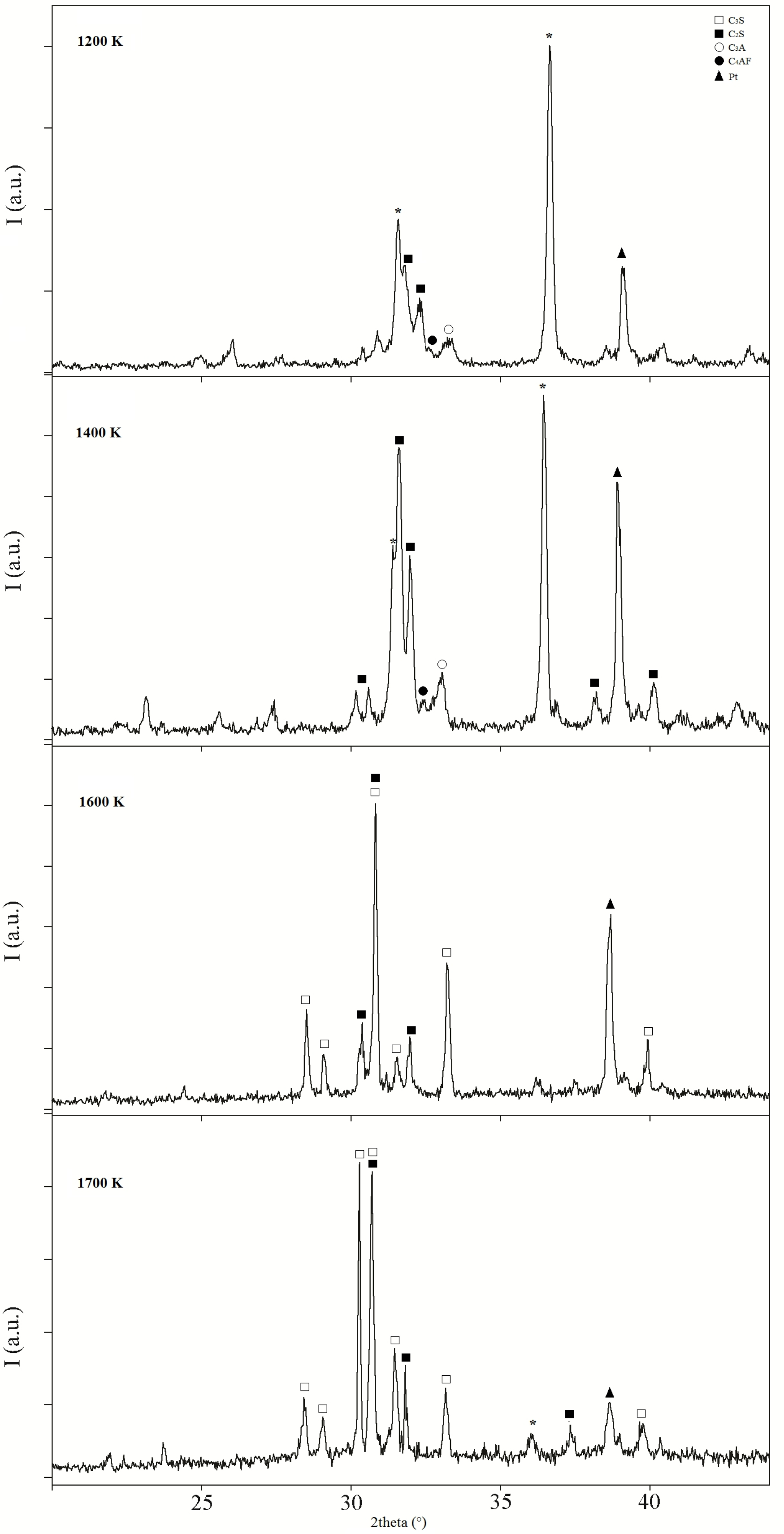

C3S
C2S
C3A
C4AF
Pt
1200 K
1400 K
1600 K
1700 K
I (a.u.)
I (a.u.)
I (a.u.)
I (a.u.)
25
30
35
40
2theta (°)

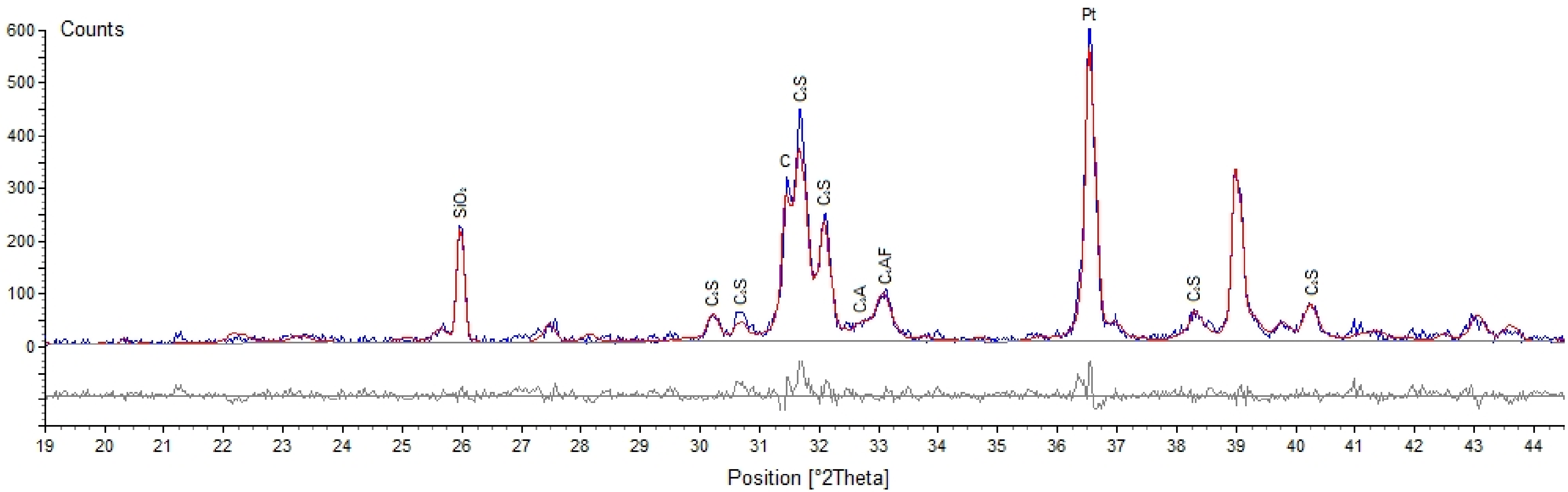

Counts
600
500
400
300
200
100
0
SiO₂
C₂S
C₂S
C
C₃S
C₃S
C₃A
C₄AF
Pt
C₂S
C₃S
19
20
21
22
23
24
25
26
27
28
29
30
31
32
33
34
35
36
37
38
39
40
41
42
43
44
Position [°2Theta]

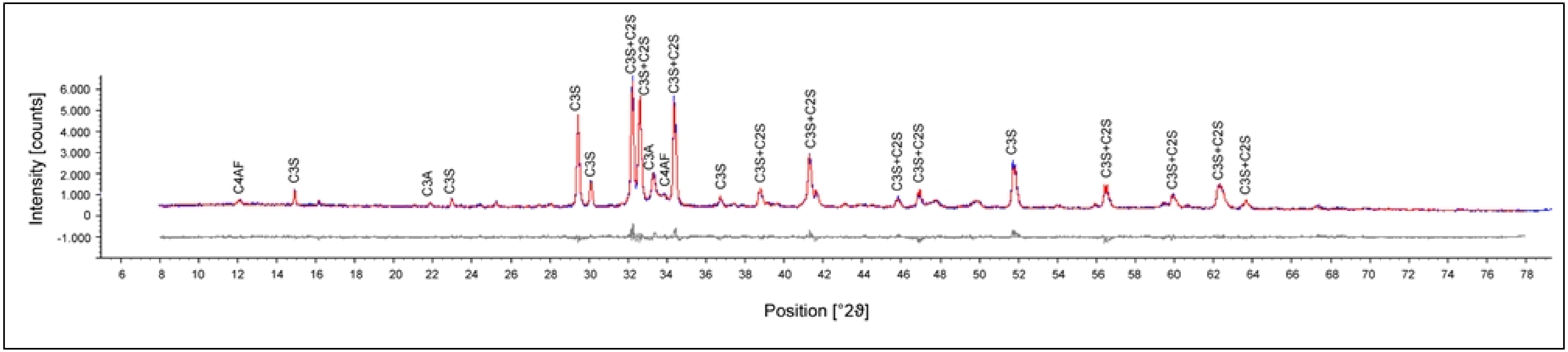

Intensity [counts]
6.000
5.000
4.000
3.000
2.000
1.000
0
-1.000
C4AF
C3S
C3A
C3S
C3S
C3S
C3S+C2S
C3S+C2S
C3A
C4AF
C3S+C2S
C3S
C3S+C2S
C3S+C2S
C3S+C2S
C3S+C2S
C3S
C3S+C2S
C3S+C2S
C3S+C2S
C3S+C2S
6 8 10 12 14 16 18 20 22 24 26 28 30 32 34 36 38 40 42 44 46 48 50 52 54 56 58 60 62 64 66 68 70 72 74 76 78
Position [°2θ]

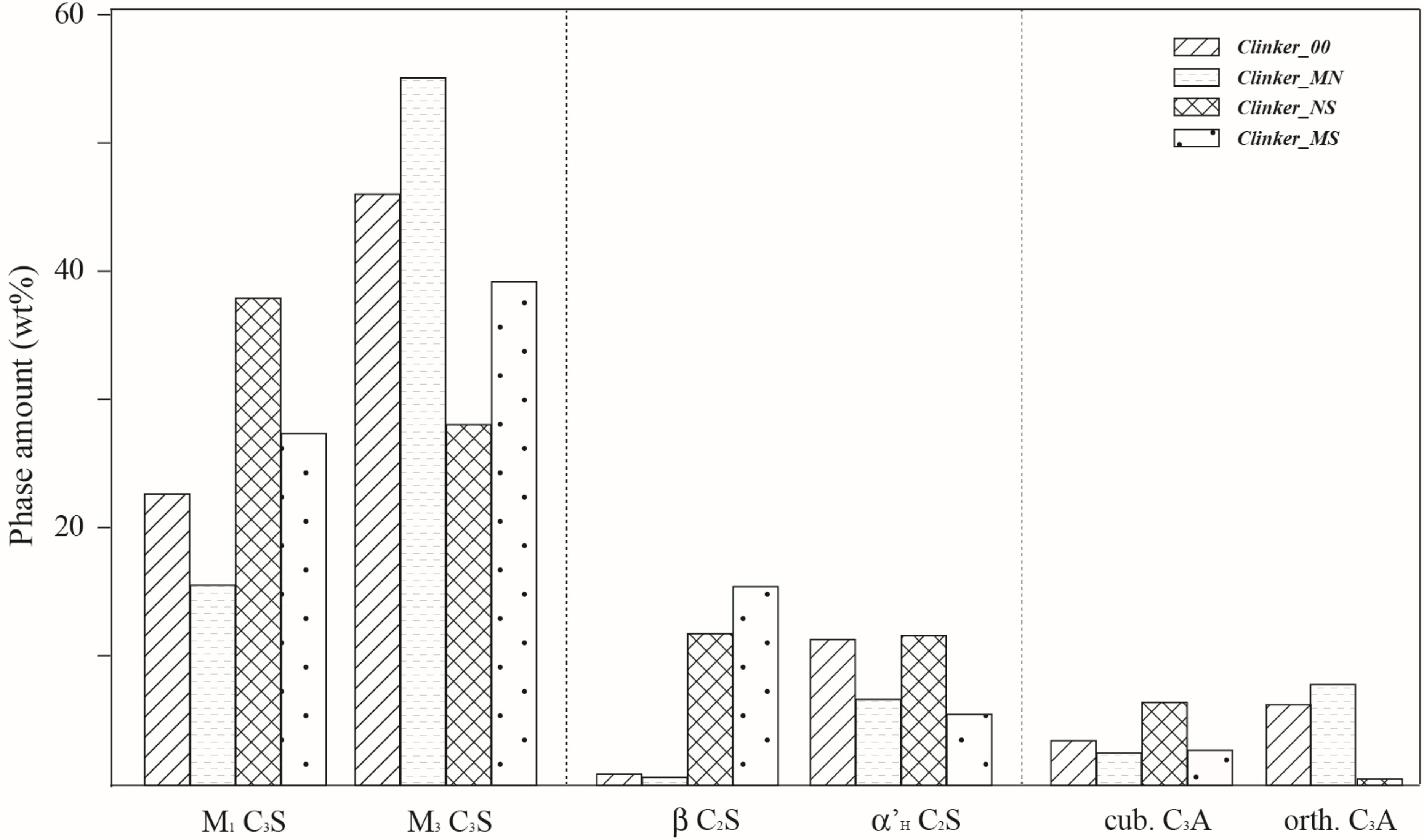

60
40
20
Phase amount (wt%)
Clinker_00
Clinker_MN
Clinker_NS
Clinker_MS
M1 C3S
M3 C3S
β C2S
α'H C2S
cub. C3A
orth. C3A

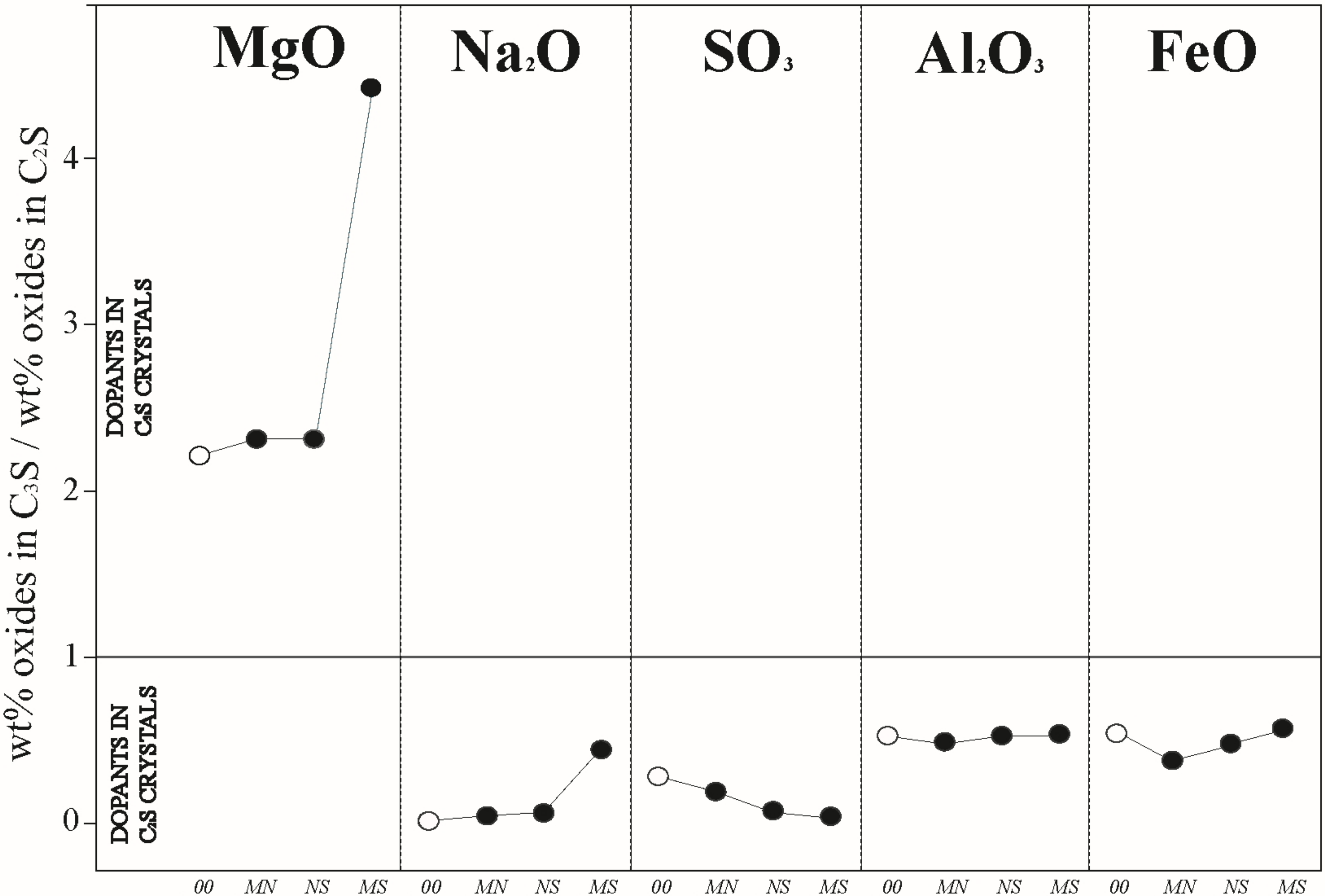

MgO
Na2O
SO3
Al2O3
FeO
wt% oxides in C3S / wt% oxides in C2S
DOPANTS IN C3S CRYSTALS
DOPANTS IN C2S CRYSTALS
0
1
2
3
4
_00
_MN
_NS
_MS

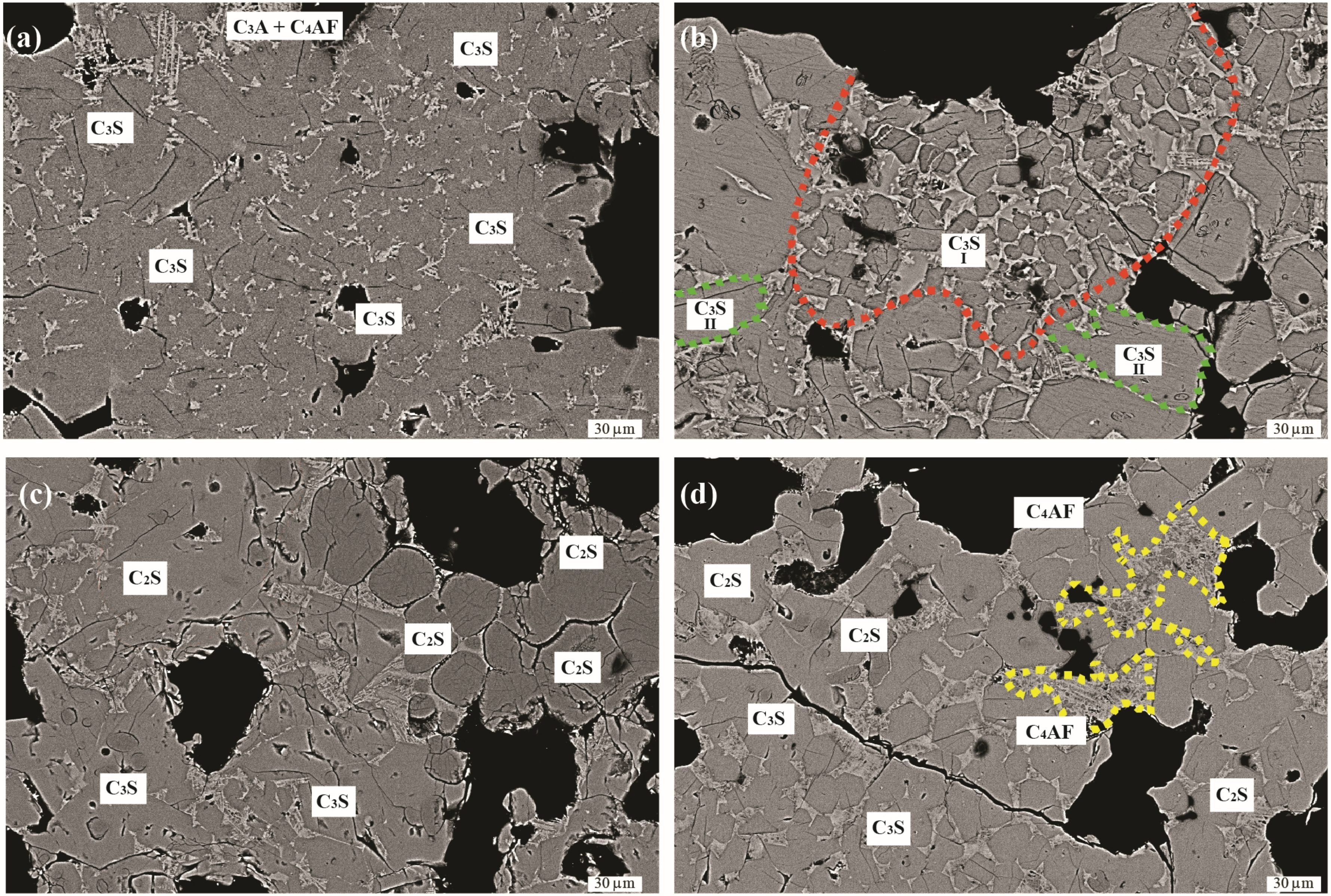

(a)
C3A + C4AF
C3S
C3S
C3S
C3S
C3S
30 μm
(b)
C3S
C3S I
C3S II
C3S II
30 μm
(c)
C2S
C2S
C2S
C2S
C3S
C3S
30 μm
(d)
C4AF
C2S
C2S
C3S
C4AF
C3S
C2S
30 μm

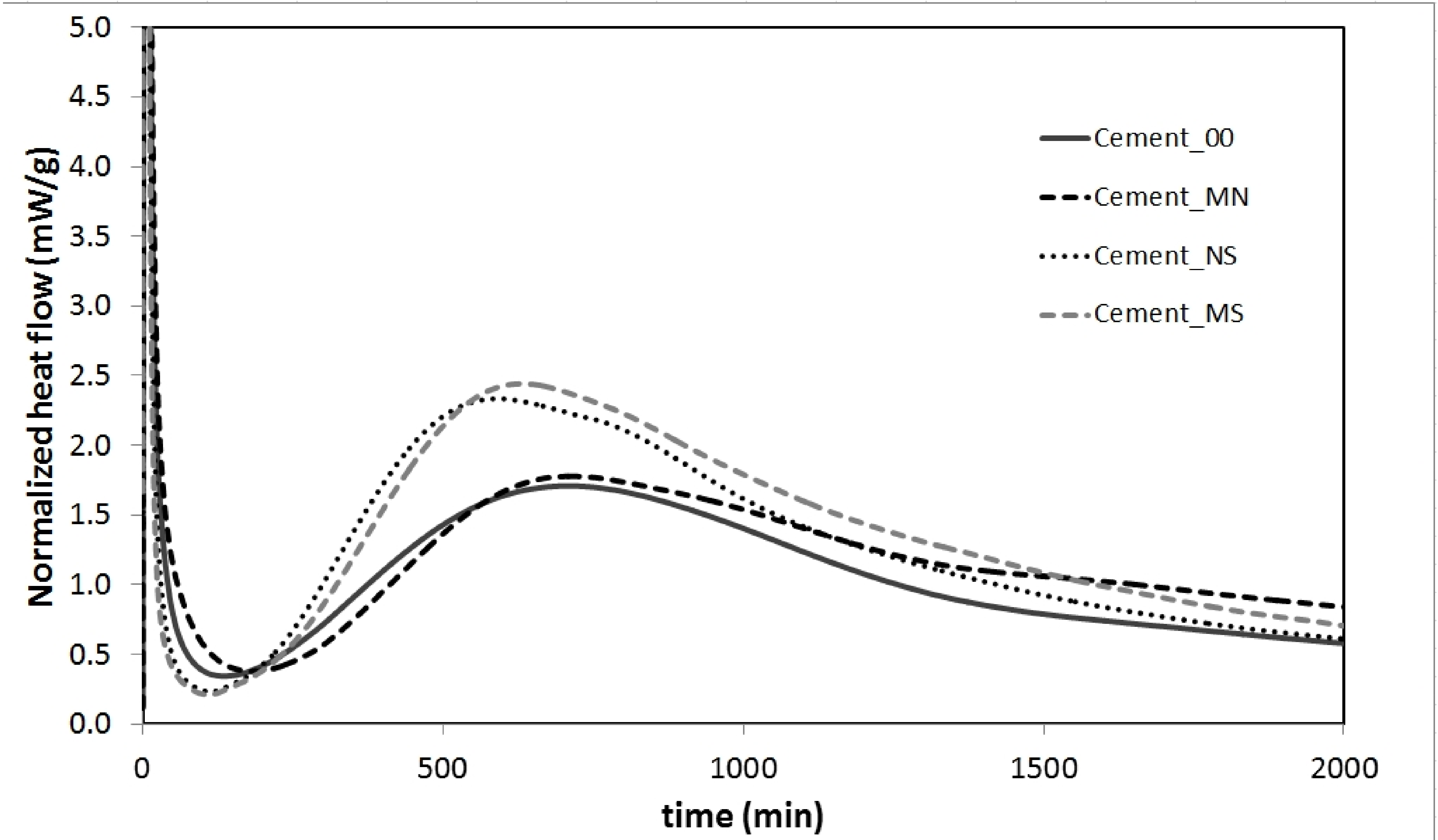

Normalized heat flow (mW/g)
5.0
4.5
4.0
3.5
3.0
2.5
2.0
1.5
1.0
0.5
0.0
0
500
1000
1500
2000
time (min)
Cement_00
Cement_MN
Cement_NS
Cement_MS

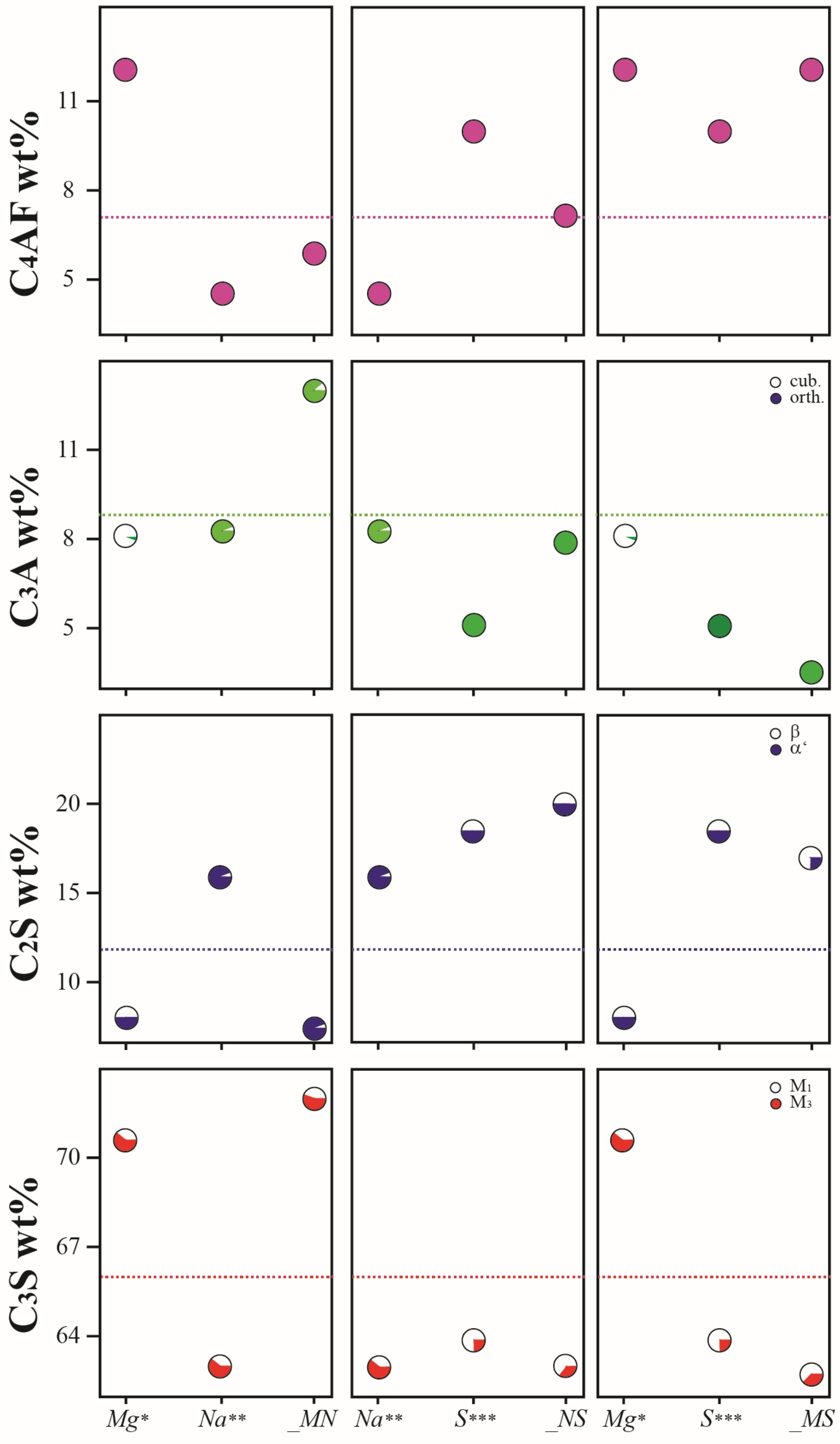

C4AF wt%
11
8
5
C3A wt%
11
8
5
cub.
orth.
C2S wt%
20
15
10
β
α'
C3S wt%
70
67
64
M1
M3
Mg*
Na**
_MN
Na**
S***
_NS
Mg*
S***
_MS